Mechanism of Methanol Synthesis on Cu(100) and Zn/Cu(100) Surfaces: Comparative Dipped Adcluster Model Study*

HIROSHI NAKATSUJI,[1,2] ZHEN-MING HU[1,†]

[1]*Department of Synthetic Chemistry and Biological Chemistry, Graduate School of Engineering, Kyoto University, Sakyo-ku, Kyoto 606-8501, Japan*
[2]*Institute for Fundamental Chemistry, 34-4 Takano-Nishihiraki-cho, Sakyo-ku, Kyoto 606, Japan*

Received 28 July 1999; accepted 29 July 1999

ABSTRACT: The mechanism of methanol synthesis from CO_2 and H_2 on Cu(100) and Zn/Cu(100) surfaces was studied using the dipped adcluster model (DAM) combined with ab initio Hartree–Fock (HF) and second-order Møller–Plesset (MP2) calculations. On clean Cu(100) surface, our calculations show that five successive hydrogenations are involved in the hydrogenation of adsorbed CO_2 to methanol, and the intermediates are formate, dioxomethylene, formaldehyde, and methoxy. The rate-limiting step is the hydrogenation of formate to formaldehyde, and the Cu–Cu site is responsible for the reaction on Cu(100). The roles of Zn on Zn/Cu(100) catalyst are to modify the rate-limiting step of the reaction: to lower the activation energies of this step and to stabilize the dioxomethylene intermediate at the Cu–Zn site. The present comparative results indicate that the Cu–Zn site is the active site, which cooperates with the Cu–Cu site to catalyze methanol synthesis on a Cu-based catalyst. Electron transfer from surface to adsorbates is the most important factor in affecting the reactivity of these surface catalysts. Int J Quant Chem 77: 341–349, 2000

Key words: dipped adcluster model; cluster model; methanol synthesis; ab initio quantum chemical methods and calculations; surface reaction; copper; zinc; carbon dioxide; hydrogenation; formate

*Dedicated to Professor Michael C. Zerner in celebration of his 60th birthday.

†*Present address:* Department of Chemistry, Dalhousie University, Halifax, Canada B3H 4J3.

Correspondence to: H. Nakatsuji.

Contract grant sponsors: Japanese Ministry of Education, Science, and Culture; Kyoto University VBL project.

CCC 0020-7608 / 00 / 010341-09

Introduction

The synthesis of methanol from syngas ($CO_2/CO/H_2$) on a Cu-based (Cu/ZnO) catalyst is one of the most extensively studied industrial processes, since it is promising not only with regard to the use of CO_2 [1, 2] but also because methanol is a key material for the synthesis of other organic materials, such as formaldehyde, alkyl halides, and acetic acids. Currently, considerable attention has been given to clarify the reaction mechanism and the nature of the active sites on the surface catalysts [3–24], with the aim of identifying a highly active and selective catalyst for methanol synthesis.

Although a satisfactory mechanism has not yet been worked out, it is now accepted that the carbon source for methanol synthesis is exclusively CO_2 [3–5], and the reaction occurs as

$$CO_2 + 3H_2 \rightarrow CH_3OH + H_2O.$$

CO may follow the water–gas shift reaction to regenerate CO_2,

$$CO + H_2O = CO_2 + H_2.$$

The mechanistic details of methanol formation from CO_2 and H_2 are not well understood. It was shown that the formate species, which is adsorbed at the bridge site with its molecular plane perpendicular to the metal surface [6–9], is a precursor involved in the methanol synthesis [5, 10]. Since several hydrogenation steps, such as the hydrogenation of CO_2, formate, and other intermediates, are involved in the actual reaction process, the identification of the intermediates and the rate-limiting step in this reaction route are the current challenging subjects. To answer some of these questions, a series of investigations has been performed for methanol synthesis using the model catalysts such as Cu(100) [11–15], Cu foil [16], Cu(110) [17], and Zn vapor-deposited copper surfaces [18–20]. The advantage of the model system is that it can give fundamental insight on the mechanism of methanol synthesis in comparison with the real Cu/ZnO catalyst. Burch et al. [10] indicated that dioxomethylene is a possible intermediate, and the critical rate-limiting step in methanol synthesis is the addition of the first hydrogen atom to Cu formate. On the other hand, Chorkendorff and co-workers [12, 13] suggested that the hydrogenation of dioxomethylene may be the rate-limiting step. The hydrogenation of formate and the hydrogenation of methoxy are also possible candidates for the rate-limiting step [13].

Regarding the active sites, early studies suggested that the copper ions (Cu^{n+}) induced by ZnO were the active site for methanol synthesis [21]. Recent studies support a model which assumes that the active site on the Cu/ZnO catalyst is metallic Cu, since the activity of the catalyst is directly proportional to the surface area of Cu [11–17]. Very recently, Nakamura and co-workers carried out a series of important studies for methanol synthesis on the Zn-deposited copper single-crystal samples [18–20]. They found that, when Zn coverage is around 0.2, the Zn-deposited Cu(111) surface is highly reactive and promotes methanol synthesis by an order of magnitude. The turnover frequency of methanol with the model catalyst agreed with that measured on real Cu/ZnO catalyst under the same reaction conditions [19]. The Cu–Zn site is then considered to be the active site, though they once suggested that Cu^{n+} species might be the active site [22–24].

Here, we give a comparative summary of our recent studies on the reaction mechanisms and the active sites of methanol synthesis on both Cu(100) and Zn/Cu(100) catalysts [34–36]. The dipped adcluster model (DAM) [25] combined with the ab initio Hartree–Fock (HF) and second-order Møller–Plesset (MP2) calculations are used. The DAM has been proposed to study chemisorptions and surface reactions by involving the interactions between bulk metal and admolecules with consideration of the electron transfer between them and the image force correction. It has been successfully applied to the chemisorption of oxygen on Pd and Ag surfaces [26–28] and the mechanisms of the epoxidation and complete oxidation of ethylene [29, 30] and propylene [31, 32] on a silver surface. A review of DAM studies has been published recently [33].

Computational Details

A $Cu_8(6,2)$ cluster, which contains six copper atoms in the first layer and two copper atoms in the second layer, as shown in Figure 1(a), was used to model the Cu(100) surface. A Cu_7Zn cluster [Fig. 1(b)] was used to model the Zn/Cu(100) alloy surface. This cluster can model the Cu–Zn bridge site reasonably and has almost the same size as the $Cu_8(6,2)$ cluster: therefore, the results on a Zn/Cu(100) surface can be compared reasonably with those on a Cu(100) surface. The DAM [25] was

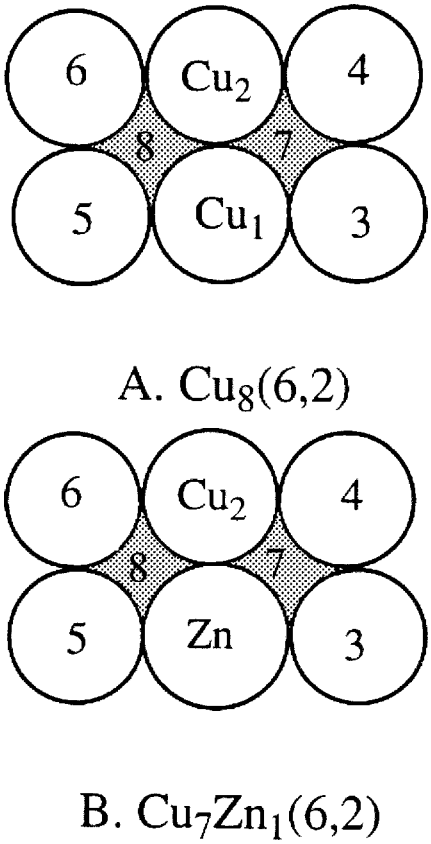

FIGURE 1. Two-layer model clusters used in this study. (a) $Cu_8(6,2)$ cluster with atoms 1–6 in the first layer and 7 and 8 in the second layer. (b) $Cu_7Zn_1(6,2)$ cluster with Zn at the bridge position of the first layer.

used to include the effects of the bulk metal, such as electron transfer between the admolecule and the surface, and the image force. The calculations were performed using the highest spin coupling model [25] and so one-electron transfer from the bulk metal was assumed [28–32].

The Langmuir–Hinshelwood (LH) mode, which corresponds to the reaction between the coadsorbed species on the surface, was assumed. The geometries of the reactants, products, and intermediates were optimized at the HF level, except for the metal–metal distances, which was fixed at its bulk lattice values [34–36]. The detailed reaction mechanism in the hydrogenation of adsorbed CO_2 to methanol was studied by choosing the appropriate bridge site reaction coordinates [34]. The electrostatic interaction energy between the adcluster and the bulk metal was estimated by the image force correction [26]. Electron correlations were included by the MP2 method. The calculations were performed using the Gaussian 94 software package [37].

The Gaussian basis set for the Cu and Zn atoms were the $(3s2p5d)/[3s2p1d]$ set and the Ar core was replaced by the effective core potential [38]. For oxygen and carbon, we used the $(9s5p)/[4s2p]$ set of Huzinaga–Dunning [39, 40]. For hydrogen, $(4s)/[2s]$ [40] was adopted in HF optimization calculations. In MP2 calculations, the polarization d function of $\alpha = 1.154$ and 0.60 [41] and the polarization p function of $\alpha = 1.1$ [37] were added to oxygen, carbon, and hydrogen, respectively. Test energetic calculations with the present methodology gave the results in reasonably good agreement with the experimental values [34].

DAM vs. Cluster Model for the Study of Coadsorption of CO_2 and H_2 and the Formate Formation on Cu(100)

Figure 2 shows a comparison between the DAM and the neutral cluster model for the optimized geometries and the energy diagrams of the coadsorption of CO_2 and H_2 and the formate formation on Cu(100). We see that the DAM can describe the coadsorption of CO_2 and H_2 and the formate formation on Cu(100). First, the DAM describes chemisorbed CO_2^- on a copper surface. In the chemisorption state, about one (0.76) electron is transferred from the bulk metal into the π^* orbital of CO_2, giving a bent anionic CO_2^- species on the surface. The C—O and O—Cu bond distances are calculated to be 1.25 and 2.15 Å, respectively. Mulliken population analysis shows that the net charge on the adsorbed species is -0.76, and the charge distribution of the metals is almost unchanged compared with that of the free cluster [34]. In the CO_2^- adsorbate, this electron transfer causes a large frontier density (spin population) on carbon, while the frontier densities on other atoms are almost zero. This large frontier density makes the carbon very reactive in the adsorption state and lets this carbon react with other coadsorbate, which is hydrogen.

On the other hand, the Cu_8 cluster model cannot describe the coadsorption of hydrogen and CO_2 on a Cu(100) surface. It is 10.2 kcal/mol more unstable, and the geometry of the CO_2 adsorbate is almost the same as that in the gas phase. If we suppose the transfer of one electron from the cluster metals to CO_2, the structure of this CO_2^- becomes similar to that [Fig. 2(a)] calculated by the DAM, but it is 33.8 kcal/mol less stable [34], and the Cu_8 cluster side has unnaturally large net charges and frontier densities. Then, the cluster is quite unstable, which

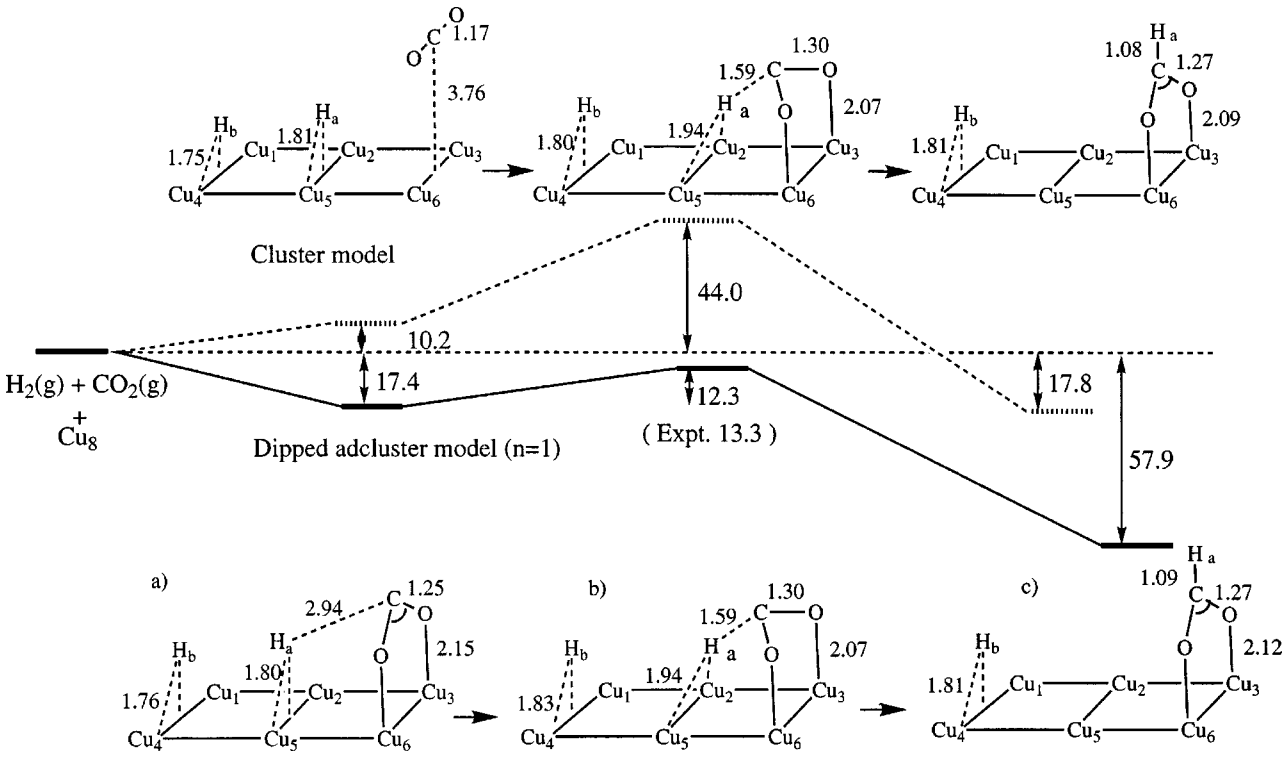

FIGURE 2. Optimized geometries and energy diagrams for the coadsorption of CO_2 and H_2, and the formate formation reaction on clean Cu(100) surface: comparison of the DAM and the neutral cluster model.

explains the large negative adsorption energy for the chemisorbed CO_2^- on the neutral cluster.

For formate formation step, the DAM calculation gives the activation energy of 12.3 kcal/mol, which is in good agreement with the experimental value of 13.3 kcal/mol [14], and this reaction step is exothermic by 40.5 kcal/mol. This means that the reaction leading to formate species is an easy reaction path, which is again in agreement with the experimental finding that formate can be easily formed on clean Cu(100) surface [11–15]. In contrast, the cluster model gives the activation energy of 44 kcal/mol and the exothermic energy of 28 kcal/mol, though the geometries are almost the same for both models. Thus, the cluster model cannot explain the formation of formate, while the DAM does it in a natural way.

The above comparative calculations show that the electron transfer from the bulk metal to the adsorbates is a key factor for the coadsorption and the reaction of H_2 and CO_2 on a copper surface. The transferred electron not only stabilize CO_2 adsorbate, but also make the central carbon to be very reactive, which initiates the series of reactions leading to methanol. Thus, the DAM is essential for theoretical studies of surface reactions in which electron transfer from the bulk metal to adsorbates is important. A similar situation was also described in the study of the roles of oxygen on a silver surface in the olefin partial oxidation reactions studied previously [27–32]. We then use the DAM to study the reaction mechanism of methanol synthesis on Cu(100) and Zn/Cu(100) surfaces.

Overall Reaction Mechanism of Methanol Synthesis on Cu(100)

One key purpose of this series of studies is to understand the mechanistic details of the series of the hydrogenation reactions on CO_2 to methanol on clean Cu(100) surface. Since it is a very complicated process, we focused on clarifying the reaction intermediates, the transition states, and the energetics of the important hydrogenation reaction step. We then determined the overall reaction mechanism as well as the rate-limiting step. The most important results and discussions are summarized in this section, but the detailed geometries and the energetics of each elementary step are described elsewhere [34].

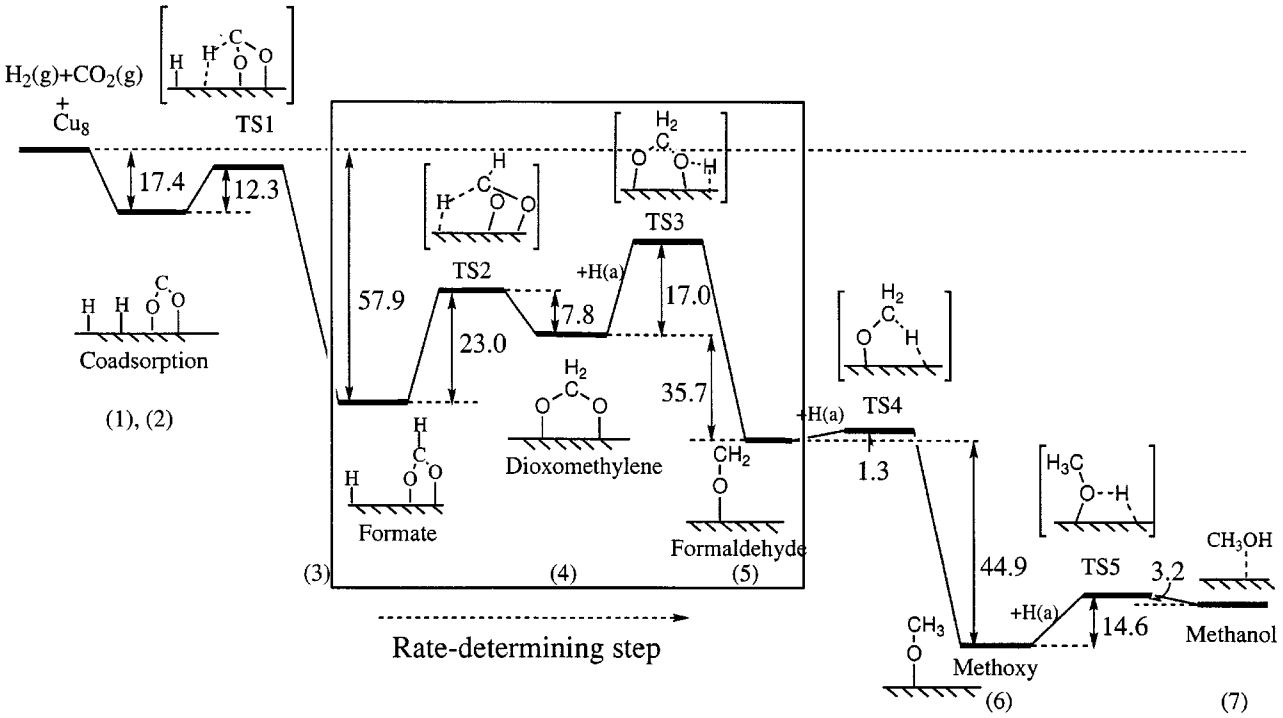

FIGURE 3. Reaction energetics for the hydrogenations of CO_2 to methanol on clean Cu(100) surface. Numbers in parentheses show the reaction steps given in the text, and the rate-limiting step is indicated by the column.

Figure 3 shows the overall reaction energetics of methanol synthesis from CO_2 and H_2 on clean Cu(100) studied by the DAM combined with the MP2 calculations. The elementary reaction steps on the surface can be summarized as follows where (g) indicates gas phase and (a) indicates adsorbed state.

$$H_2(g) \rightarrow 2H(a), \quad (1)$$
$$CO_2(g) \rightarrow CO_2(a), \quad (2)$$
$$CO_2(a) + H(a) \rightarrow HCOO(a), \quad (3)$$
$$HCOO(a) + H(a) \rightarrow H_2COO(a), \quad (4)$$
$$H_2COO(a) + H(a) \rightarrow H_2CO(a) + OH(a), \quad (5)$$
$$H_2CO(a) + H(a) \rightarrow H_3CO(a), \quad (6)$$
$$H_3CO(a) + H(a) \rightarrow CH_3OH, \quad (7)$$
$$OH(a) + H(a) \rightarrow H_2O. \quad (8)$$

Among these elementary reactions, (3)–(7) constitute the core steps in methanol synthesis as shown in Figure 3. The energy diagram shown in Figure 3 is composed of the energetics of the elementary reaction steps [34] and gives an intuitive understanding of the reaction pathway. It is noted that since the composition of hydrogen varies in the reaction steps, an energy comparison among the different steps may have little meaning, except for the activation energy. Figure 3 is to provide an overview of the reaction mechanism in methanol synthesis based on our theoretical studies [34].

Among the hydrogenation steps, the hydrogenation of adsorbed formate giving adsorbed dioxomethylene, i.e., step (4), is the rate-limiting step, as shown in Figure 3. The activation energy of this step is calculated to be 23.0 kcal/mol, which is higher than that in other hydrogenation steps. This step is also endothermic by 17.1 kcal/mol. This result is consistent with the suggestion based on experimental findings that the critical rate-limiting step in methanol synthesis is the addition of the first hydrogen atom to adsorbed formate [5, 10, 16]. The high-energy barrier and an unstable dioxomethylene intermediate account for the lower activity of a clean copper surface as compared with a Cu-based catalyst in practical methanol synthesis. Dioxomethylene has been suggested to be an intermediate in methanol synthesis [10, 13], but there is no direct experimental evidence to confirm this point. Our optimization calculations show that dioxomethylene is adsorbed on a Cu(100) surface at the bridge site with its molecular plane perpendicular to the metal surface; i.e., an adsorption geometry similar to that of formate adsorbed on the surface.

Another high-energy barrier (17 kcal/mol) is calculated for step (5), the hydrogenation of adsorbed dioxomethylene to give formaldehyde, while this step is exothermic by 35.7 kcal/mol. Therefore, step (5) may cooperate with step (4) to be rate-limiting, though the former seems be easier than the latter. Experimentally, Chorkendorff and coworkers [12, 13] suggested that step (5) may be rate-limiting. On the other hand, the decomposition of dioxomethylene into formate, i.e., the backward reaction, is also favorable: The energy barrier is 5.9 kcal/mol and the reaction is exothermic by 17.1 kcal/mol. One can expect that dioxomethylene will decompose into formate in the absence of coadsorbed hydrogen. Thus, step (5) is important for achieving a high selectivity in methanol synthesis: It is more reasonable to say that the formate to formaldehyde reactions [steps (4) and (5)] are the rate-limiting steps. Compared with steps (4) and (5), steps (6) and (7) are both easy and rapid, leading to an overall exothermic methanol synthesis.

Our calculations show that chemisorbed CO_2^-, formate, dioxomethylene, formaldehyde, and methoxy are the main intermediates in methanol synthesis, and Eqs. (3)–(7) provide a reasonable reaction route leading to methanol formation on a Cu(100) surface. Surface formate is readily formed by the reaction of adsorbed atomic hydrogen with coadsorbed CO_2, which exists as a bent anionic CO_2^- species. About one electron is transferred from the metal surface to the π^* orbital of CO_2, making the carbon very reactive. Adsorbed formate is easily synthesized from CO_2 and H_2 on a Cu(100) surface [10, 14], as has been shown experimentally. Adsorbed formate has been confirmed to be a reaction intermediate by infrared [5, 42] and temperature programmed desorption (TPD) [43] experiments.

Roles of the Zn–Cu Site in the Rate-Limiting Step: Comparison with Cu(100)

As shown above, the rate-limiting step in methanol synthesis is clarified to be the steps (4) and (5). Figure 4 shows the energy diagrams of these steps on a Zn/Cu(100) alloy surface in comparison with those on a clean Cu(100) surface: the hydrogenation of formate to dioxomethylene involving transition state 2 (TS2) and the hydrogenation of dioxomethylene to formaldehyde involving TS3. The Cu–Cu site of the Cu(100) catalyst and the Cu–Zn site of the Zn/Cu(100) catalyst are both responsible for these reaction steps, and the reaction mechanisms are essentially the same and comparative between the two catalyst surfaces [35].

The differences between the two energy diagrams are evident. On a Cu(100) catalyst, the activation energy of step (4) was calculated to be 23 kcal/mol, and the dioxomethylene is endothermic by 17.1 kcal/mol. The next step [step (5)] has an activation energy of 17 kcal/mol. The experimental activation energy for the hydrogenation of formate on a Cu(100) surface was reported to be 19.6 kcal/mol [15]. The relatively large energy barriers in steps (4) and (5) and an unstable dioxomethylene intermediate at the Cu–Cu site indicate a slow reaction rate and explain low activity of the clean Cu(100) catalyst. On the other hand, on the Zn/Cu(100) catalyst, the activation energy of step (4) was calculated to be 8.5 kcal/mol, and it is exothermic by 2.7 kcal/mol. The dioxomethylene intermediate formed at the Cu–Zn site is 7.4 kcal/mol more stable than that at the Cu–Cu site. Formate on the Cu–Cu site migrates onto the Cu–Zn site to pass through the lower activation barrier leading to dioxomethylene. The activation energy of step (5) at the Cu–Zn site is 11.5 kcal/mol, which is again lower than 17 kcal/mol for the same reaction at the Cu–Cu site. All these results indicate that the Cu–Zn site on a Zn/Cu(100) catalyst cooperates with the Cu–Cu site to make the reaction easier and works as the active site for the hydrogenation of formate to formaldehyde, the rate-limiting step in methanol synthesis.

Another interesting feature of the results is that the formate and the formaldehyde species adsorbed at the Cu–Zn site are calculated to be less stable than that at the Cu–Cu site. Since the adsorbates prefer to occupy the most stable site on the surface, most of them will be adsorbed at the Cu–Cu site. The Cu–Cu site should play an important role in formate formation and in the reaction process of formaldehyde to methanol product. Indeed, these reaction steps are previously calculated to proceed much easier than the rate-limiting step on clean Cu(100) surface [34].

The above results provide a clear understandable reaction mechanism for methanol synthesis on the Zn-deposited copper catalysts. CO_2 reacts with hydrogen on the catalysts to produce the adsorbed formate intermediate. Formate adsorbed at the Cu–Cu site can be hydrogenated into dioxomethylene with a relatively higher activation energy. On the Zn-deposited copper catalyst, the Cu–Zn alloy sites are formed by substitution of Zn atoms with the Cu

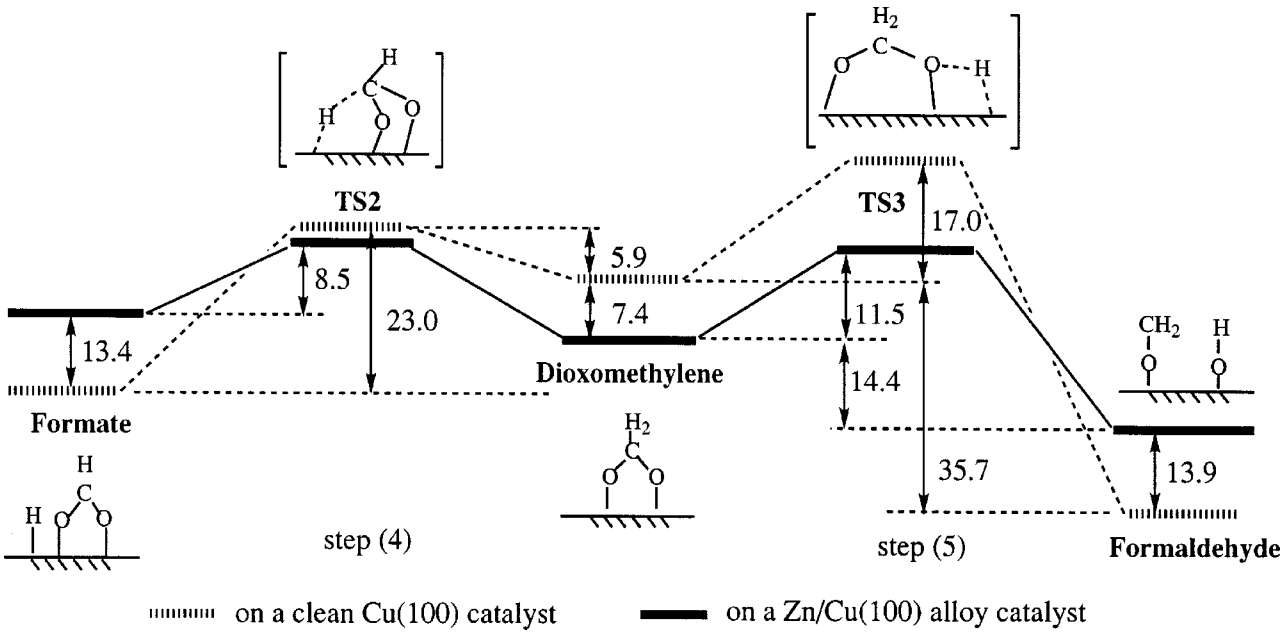

FIGURE 4. Energy diagram for the rate-limiting hydrogenation steps (4) and (5) on the model Zn/Cu(100) alloy catalyst (solid line) and on the model Cu(100) clean catalyst (dashed line).

surface atoms as confirmed by the experimental scanning tunneling microscopy (STM) images [44]. Since dioxomethylene intermediate at the Cu–Zn site is more stable and reactive than that on the Cu–Cu site, formate on the Cu–Cu site will migrate onto the Cu–Zn site and is hydrogenated into dioxomethylene via a lower transition state. The hydrogenation of dioxomethylene to formaldehyde will proceed mainly at the Cu–Zn site because of the existence of a low-energy path. The formaldehyde product at the Cu–Zn site will then migrate back to the Cu–Cu site due to a larger stability. As a result, both the Cu–Zn and Cu–Cu sites are important, and they cooperate with each other to realize high reactivity in methanol synthesis. The Cu–Zn site provides an active site for the rate-limiting step and hence enhance the activity of the catalysts. As pointed out in a previous study [34], a key to enhance the overall reactivity in methanol synthesis is to design the catalyst which stabilizes the dioxomethylene intermediate and works to lower the energy barrier in the hydrogenation of formate. The Cu–Zn site on the Zn-deposited copper catalyst plays just such a role and explains the high reactivity reported experimentally [18–20].

The electronic origin of the higher reactivity of Zn/Cu(100) catalyst as compared with Cu(100) catalyst is explained from the difference in the electronic properties of Zn and Cu. Since all the adsorbates are the electron-withdrawing species, the charge-transfer ability of the catalyst appears to be the main factor in affecting the reactivity. The Zn atom of the Zn/Cu(100) catalyst shows different electronic state from the Cu atoms: Though Cu is in a neutral metallic state, the Zn atom is almost in the ionic Zn^+ state. Therefore, Zn acts as an electron source and modifies the electronic properties of the catalyst to realize a larger charge-transfer ability. Our calculation shows that in the rate-limiting step, the adsorbates have larger negative charges on the Zn–Cu site than on the Cu–Cu site [35]. This confirms that the Zn-deposited copper catalyst has larger charge-transfer ability and affects the reactivity of the catalysts toward methanol synthesis by affecting the most significant rate-limiting reaction steps (4) and (5). The facts that the promoter modifies the electronic properties of the metal surface and hence affect the reactivity have been reported for the reactions of S_2 and O_2 with metallic Cu and Cu/ZnO by Rodriguez et al. [45, 46]. It is also noteworthy that, in the rate-limiting reaction step, the O—Zn bond distance is calculated to be shorter than the O—Cu bond distance. The O–Zn interaction is then stronger than the O–Cu interaction, another difference of the Zn/Cu(100) catalyst in comparison with the Cu(100) catalyst. More details about the geometries and the electronic properties

of the reaction species on the Zn/Cu(100) catalyst will be described elsewhere [36].

Conclusions

The reaction mechanism and the active sites for methanol synthesis from CO_2 and H_2 on Cu(100) and Zn/Cu(100) surfaces are clarified by using the dipped adcluster model (DAM) combined with ab initio HF and MP2 calculations.

On clean Cu(100) surface, our calculations show that five successive hydrogenations are involved in the course of the methanol synthesis from CO_2 and H_2: The intermediates are formate, dioxomethylene, formaldehyde, and methoxy. The rate-limiting step is the hydrogenation of adsorbed formate leading to formaldehyde with dioxomethylene intermediate, and the Cu–Cu site is responsible for the reaction on Cu(100).

The effects of Zn on a Zn/Cu(100) catalyst are to modify the rate-limiting step of the reaction, and the roles are twofold: One is to lower the activation energies of the hydrogenation reactions of formate and dioxomethylene, and another is to stabilize the dioxomethylene intermediate at the Cu–Zn site. The role of the Cu–Zn site is then to enhance the reactivity of the adsorbed formate and dioxomethylene species, and then acts as an active site in methanol synthesis.

The formate and formaldehyde species at the Cu–Cu site are more stable than that at the Cu–Zn site. Except for the rate-limiting step, other reaction steps of methanol synthesis would proceed on the Cu–Cu site. Therefore, for overall methanol synthesis both Cu–Zn and Cu–Cu sites are important and cooperate for smooth overall progress of the series of the reactions.

Electron transfer is an important key feature in this catalytic reaction processes. The DAM is then an appropriate model. All the adsorbates are anionic on the surface, and the role of Zn is to modify the electronic properties of the Zn/Cu(100) catalyst so as to realize larger electron transfers. This is the main factor which is responsible for the high reactivity of the formate and dioxomethylene on a Zn/Cu(100) catalyst.

ACKNOWLEDGMENTS

We celebrate the 60th birthday of Professor Michael C. Zerner who has made pioneering studies in many different fields of chemistry, in particular, excited-state chemistry, biological chemistry, and catalytic chemistry which are the fields in which we have long shared common interests and exchanged our sciences. Some of the calculations of this study were performed using the computers at the Institute for Molecular Science. Part of this study was supported by a Grant-in-Aid for Scientific Research from the Japanese Ministry of Education, Science, and Culture and by a grant from the Kyoto University VBL project.

References

1. Saito, M. Shokubai (Catalyst) 1993, 35, 485, in Japanese.
2. Chinchen, C. G.; Denny, P. J.; Jennings, J. R.; Spencer, M. S.; Waugh, K. C. Appl Catal 1988, 36, 1.
3. Bowker, M.; Houghton, H.; Waugh, K. C. J Chem Soc Faraday Trans 1981, 77, 3023.
4. Chinchen, G. C.; Denny, P. J.; Parker, D. G.; Spencer, M. S.; Waugh, K. C.; Whan, D. A. Appl Catal 1987, 30, 333.
5. Millar, G. J.; Rochester, C. H.; Waugh, K. C. Catal Lett 1992, 14, 289.
6. Woodruff, D. P.; McConville, C. F.; Kilcoyne, A. L. D.; Linder, Th.; Somers, J.; Surman, M.; Paolucci, G.; Bradshaw, A. M. Surf Sci 1988, 201, 228.
7. Mehandru, S. P.; Anderson, A. B. Surf Sci 1989, 219, 68.
8. Wander, A.; Holland, B. W. Surf Sci 1988, 199, L403.
9. Casarin, M.; Granozzi, G.; Sambi, M.; Tondello, E.; Vittadini, A. Surf Sci 1994, 315, 309.
10. Burch, R.; Golunski, S. E.; Spenser, M. S. Catal Lett 1990, 5, 55.
11. Szanyi, J. S.; Goodman, W. Catal Lett 1991, 10, 383.
12. Rasmussen, P. B.; Kazuta, M.; Chorkendorff, I. Surf Sci 1994, 318, 267.
13. Rasmussen, P. B.; Holmblad, P. M.; Askgaard, T.; Ovesen, C. V.; Stoltze, P.; Nørskov, J. K.; Chorkendorff, I. Catal Lett 1994, 26, 373.
14. Taylor, P. A.; Rasmussen, P. B.; Ovesen, C. V.; Stoltze, P.; Chorkendorff, I. Surf Sci 1992, 261, 191.
15. Chorkendorff, I.; Taylor, P. A.; Rasmussen, P. B. J Vac Sci Technol A 1992, 10, 2277.
16. Yoshihara, J.; Parker, S. C.; Schafer, A.; Campbell, C. T. Catal Lett 1995, 31, 313.
17. Yoshihara, J.; Campbell, C. T. J Catal 1996, 161, 776.
18. Nakamura, I.; Nakano, H.; Fujitani, T.; Uchijima, T.; Nakamura J. Surf Sci 1998, 402, 92.
19. Fujitani, T.; Nakamura, I.; Uchijima, T.; Nakamura, J. Surf Sci 1997, 383, 285.
20. Nakamura, I.; Fujitani, T.; Uchijima, T.; Nakamura, J. Surf Sci 1998, 383, 387.
21. Klier, K. Adv Catal 1982, 31, 243.
22. Fujitani, T.; Nakamura, I.; Uchijima, T.; Nakamura, J. Surf Sci 1994, 285, 285.
23. Kanai, Y.; Watanabe, T.; Fujitani, T.; Uchijima, T.; Nakamura, J. Catal Lett 1996, 38, 157.
24. Nakamura, J.; Nakamura, I.; Uchijima, T.; Kanai, Y.; Watanabe, T.; Saito, M.; Fujitani, T. J Catal 1996, 160, 65.

25. Nakatsuji, H. J Chem Phys 1987, 87, 4995.
26. Nakatsuji, H.; Nakai, H.; Fukunishi, Y. J Chem Phys 1991, 95, 640.
27. Nakatsuji, H.; Nakai, H. J Chem Phys 1993, 98, 2423.
28. Nakatsuji, H.; Hu, Z-M.; Nakai, H.; Ikeda, K. Surf Sci 1997, 387, 328.
29. Nakatsuji, H.; Nakai, H.; Ikeda, K.; Yamamoto, Y. Surf Sci 1997, 384, 315.
30. Nakatsuji, H.; Takahashi, K.; Hu, Z-M. Chem Phys Lett 1997, 277, 551.
31. Hu, Z-M.; Nakai, H.; Nakatsuji, H. Surf Sci 1998, 401, 371.
32. Nakatsuji, H.; Hu, Z-M.; Nakai, H. Int J Quant Chem 1997, 65, 839.
33. Nakatsuji, H. Prog Surf Sci 1997, 54, 1.
34. Hu, Z. M.; Takahashi, K.; Nakatsuji, H. Surf Sci 1999, in press.
35. Hu, Z. M.; Nakatsuji, H. Chem Phys Lett 1999, in press.
36. Hu, Z. M.; Nakatsuji, H., to appear.
37. Frish, M. J.; Trucks, G. W.; Schlegel, H. B.; Gill, P. M. W.; Johnson, B. G.; Robb, M. A.; Cheeseman, J. R.; Keith, T. A.; Petersson, G. A.; Montgomery, J. A.; Raghavachari, K.; Al-Laham, M. A.; Zakrzewski, V. G.; Ortiz, J. V.; Foresman, J. B.; Cioslowski, J.; Stefanov, B. B.; Nanayakkara, A.; Challacombe, M.; Peng, C. Y.; Ayara, P. Y.; Chen, W.; Wong, M. W.; Andres, J. L.; Replogle, E. S.; Gomperts, R.; Martin, R. L.; Fox, D. J.; Binkley, J. S.; Defrees, D. J.; Baker, J.; Stewart, J. P.; Head-Gordon, M.; Gonzales, C.; Pople, J. A.; Gaussian 94 (Revision E.2), Gaussian, Inc., Pittsburgh, 1995.
38. Hay, P. J.; Wadt, W. R. J Chem Phys 1985, 82, 270.
39. Huzinaga, S. J Chem Phys 1965, 42, 1293.
40. Dunning, Jr., T. H. J Chem Phys 1970, 53, 2823.
41. Huzinaga, S.; Andzelm, J.; Kiobukowski, M.; Radzio-Andzelm, E.; Sakai, Y.; Tatewaki, H., Gaussian Basis Sets for Molecular Calculations, Physical Science Data, Vol. 16; Elsevier: Amsterdam, 1984, p. 23.
42. Kiennemann, A.; Idriss, J.; Hindermann, J. P.; Lavalley, J. C.; Vallet, A.; Chaumette, P.; Courty, P. H. Appl Catal 1990, 59, 165.
43. Bowker, M.; Hadden, R. A.; Houghton, H.; Hyland, J. N.; Waugh, K. C. J Catal 1988, 109, 263.
44. Nakamura, J.; Nakamura, I.; Uchijima, T.; Watanabe, T.; Fujitani, T. Stud Surf Sci Catal 1996, 101, 1389.
45. Rodriguez, J. A.; Chaturvedi, S.; Kuhn, M. Surf Sci 1998, 415, L1065.
46. Chaturvedi, S.; Rodriguez, J. A.; Hrbek, J. J Phys Chem B 1997, 101, 10860.